

# A systematic FEM analysis of the influence of mechanical properties in the reliability of the correlation methods in the Small Punch Test

Jose Calaf-Chica<sup>(1)</sup>, Pedro Miguel Bravo Díez<sup>(2)</sup>, Mónica Preciado Calzada<sup>(3)</sup>, Daniel Ballorca-Juez<sup>(4)</sup>

*E-mails: (1) Corresponding author, jcalaf@ubu.es ; (2) pmbravo@ubu.es; (3) mpreciado@ubu.es; (4) dbj0001@alu.ubu.es  
Postal address: Departamento de Ingeniería Civil, Universidad de Burgos, Avenida Cantabria s/n, E09006 Burgos, Spain*

## ABSTRACT

The Small Punch Test (SPT) is a miniature mechanical characterization test used as an alternative method to obtain a wide selection of mechanical properties (Young's modulus, yield strength, ultimate tensile strength, fracture toughness, etc). These mechanical properties are obtained in the SPT from correlations with different data of the load-displacement curve of the test (SPT curve). The main disadvantage of the SPT is the scattering observed when a wide set of materials is included in the correlations. A systematic finite element analysis of the SPT was performed for an extensive selection of hypothetical materials with an extensive range of mechanical properties (Young's modulus, yield strength and strain hardening) in order to study the influence of each mechanical property on the correlation methods. This investigation showed the multi-dependencies of the current correlation methods with more than one mechanical property. These multiple dependencies were analyzed and quantified and were introduced in the correlation equations to reduce the scattering.

**Keywords:** Small Punch Test, SPT, yield strength, ultimate tensile strength, strain-hardening.

**Note:** No specific grants from funding agencies in the public, commercial, or non-profit sectors were received.

## 1 Introduction

In the early 80's the nuclear industry was looking for the influence of irradiation on the mechanical properties of steels. It was necessary to perform a large number of tests, but the required time to irradiate the standard tensile specimens was too long for the industrial demand. In the multiple research lines motivated by this issue, the Miniaturized Disk Bend Test (MDBT) was introduced by Manahan in 1981 [1,2]. During the 80's the MDBT resulted in other alternatives: bulge test [3], shear punch test [4] and the small punch test (SPT) [5] and, in the 90's, the SPT turned into the most accepted test by the researchers.

Initially the SPT was used to measure the influence of irradiation on the ductility of steels [6], and nowadays it has been extended to other mechanical properties: Young's modulus [7,8], yield strength [9,10], ultimate tensile strength [11], ductile-to-brittle transition temperature [5], fracture properties [12] and creep behavior [13]. The CEN Code of Practice CWA 15627 was introduced in 2006 and revised in 2007 [14] to standardize the SPT. Following this, the publication of European Standard for the SPT in 2019 is planned [15].

The geometry and the setup of the SPT are represented schematically in Figure 1. The specimen is a plain disk with an outer diameter larger than 8.0 mm and a thickness of  $t = 0.5$  mm. It is clamped between two dies and punched by a hemispherical part with radius of  $R_p = 1.25$  mm. The lower die has an inner hole with a radius of  $R_d = 2.0$  mm and a fillet radius of  $r = 0.5$  mm. During the test, the specimen is loaded and deformed by the punch until failure and the load vs. displacement data are registered. The curve obtained is known as the SPT curve (see Figure 2).

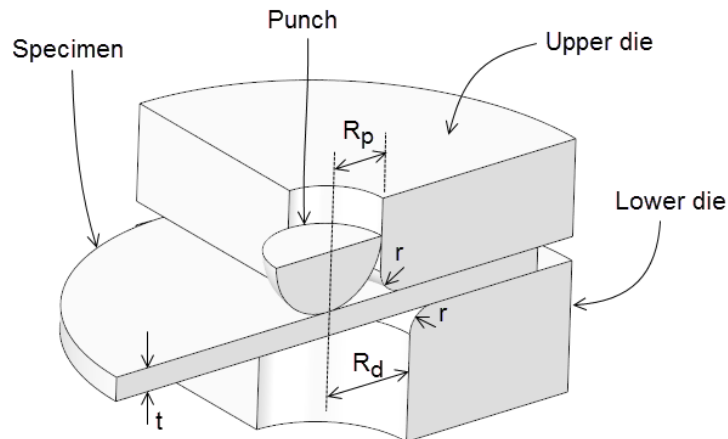


**Figure 1.** SPT set up

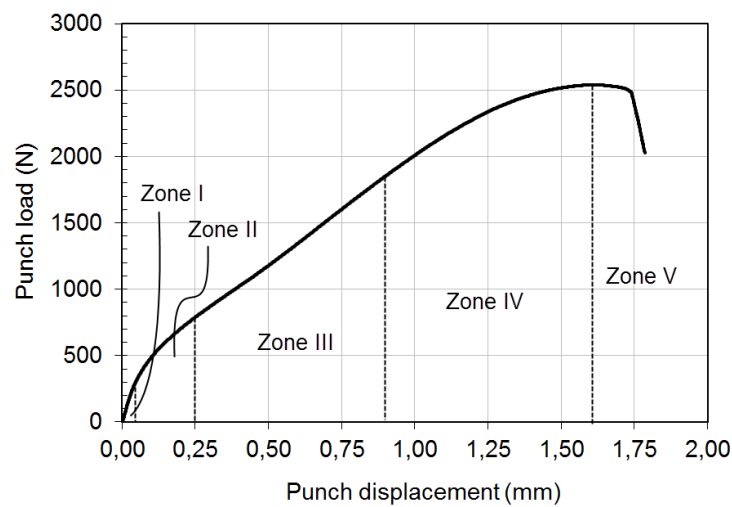


**Figure 2.** Experimental SPT curve

The SPT curve is divided in five behavior zones (see Figure 2):

- Zone I. Elastic bending of the specimen.
- Zone II. Transition from elastic bending to plastic bending.
- Zone III. Plastic hardening.
- Zone IV. Softening due to necking and damage initiation.
- Zone V. Crack growth and failure of the specimen.

The mechanical properties inherent to the standard tensile test (Young's modulus, yield strength and ultimate tensile strength) are obtained through the correlations of the data extracted from the SPT curve for each mechanical property. From 80's a large variety of correlation methods were introduced for the characterization of the three mechanical properties pointed out previously.

There are two methodologies to correlate the Young's modulus:

- a) Initial slope method [7]. Introduced by Fleury et al., this method correlated linearly the initial slope of the zone I of the SPT curve with the Young's modulus of the material. The zone I of the SPT curve shows a non-linear behavior with an inflection point and a maximum slope named as  $Slope_{ini}$ , which is used in this correlation method.

- b)  $Slope_{UL}$  method [8]. This correlation method introduced an unloading-loading cycle (UL cycle) at a fixed punch displacement of 0.1 mm. The mean value of the slope during the loading step of this UL cycle was correlated with the Young's modulus showing lower deviations than the Initial slope method.

The yield strength has been the most studied mechanical property in the SPT. Although there are up to eight methods [17], three of them are the most accepted correlation methods:

- a) Mao's method or two tangents' method [9].
- b) CEN's method [14].
- c) Offset  $t/10$  method [10].

Mao's method (see Figure 3): two tangents, one in the maximum slope of the zone I ( $Slope_{ini}$ ) and the second one in the minimum slope of the zone III ( $Slope_{min}$ ), are calculated to obtain the crossing point between them. The load of this point is named as yield load ( $P_y$ ). The estimation of the yield strength with this yield load needs to perform SPT's and standard tensile tests in a set of materials. Each pair of yield load and yield strength is plotted in a graph and all of them correlated linearly with the following equation (1).

$$\sigma_y = \alpha_1 \frac{P_y}{t^2} + \alpha_2 \quad (1)$$

where:

$\alpha_1$  and  $\alpha_2$  are correlation coefficients obtained in the linear regression.  
 $t$  is the specimen thickness.

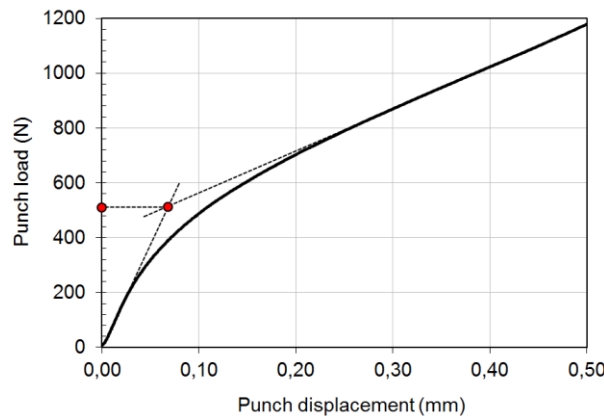


**Figure 3.**  $P_y$  calculation with the Mao's method

CEN's method (see Figure 4): the CEN Code of Practice CWA 15627 introduced this correlation method, which used a discontinuous function  $f(u)$  made up of two straight lines. To calculate this function, an error equation must be minimized. The point A is defined as the crossing point between both lines. The y-value of the projection of A on the SPT curve is taken as the yield load  $P_y$ , which is linearly correlated with the yield strength following the equation (1). The European Standard for the SPT, which will be published in 2019, will modify the CEN method using the load of the crossing point A instead of the vertical projection [15]. Thus, this future modification was used in this investigation instead of the practice established in the CWA 15627.

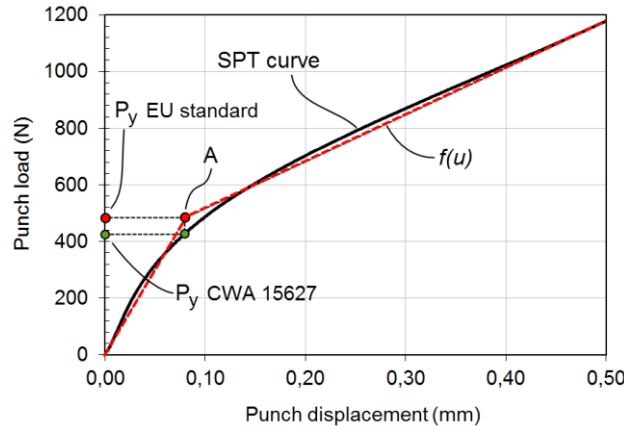


**Figure 4.**  $P_y$  calculation with the CEN's method

Offset  $t/10$  method (see Figure 5): the yield load  $P_y$  is obtained in a similar way as for the standard tensile test. An offset line of  $t/10$ , parallel to the maximum slope of the zone I of the SPT curve ( $Slope_{ini}$ ) is drawn. The load of the crossing point between this offset line with the SPT curve corresponds to the yield load  $P_y$  used to correlate linearly with the yield strength. The correlation equation is similar to equation (1).

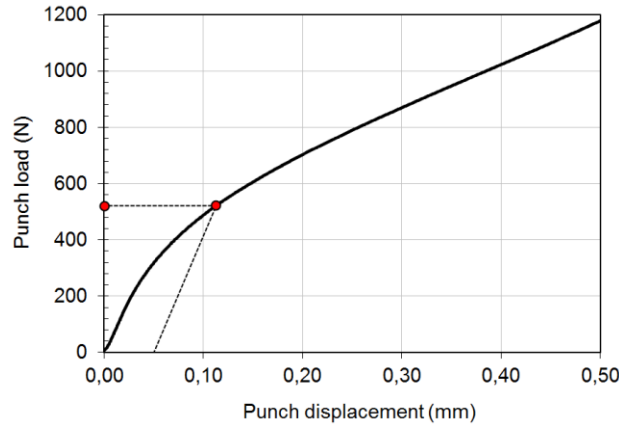


**Figure 5.**  $P_y$  calculation with the offset  $t/10$  method

Recently, a new correlation method for the yield strength was introduced in 2017 [16]: the  $Slope_{ini}$  method. This used the maximum slope of the zone I of the SPT curve ( $Slope_{ini}$ ) and correlated it with the yield strength. This method showed, numerically and experimentally, lower deviations than the current correlation methods. The main weakness of this method was the dependency of the  $Slope_{ini}$  with the Young's modulus. That is why this research focused only on steels.

For the ultimate tensile strength correlation with the SPT, there are three methods:

- a) Maximum load  $P_m$  method [11].
- b) Maximum load  $P_m$  method balanced with displacement  $u_m$  [18].
- c) Intersections' method [19].

Maximum load method (see Figure 6): this correlation method is based on the use of the maximum load  $P_m$  of the SPT curve to obtain the ultimate tensile strength. This maximum load  $P_m$  is correlated linearly with the next equation (2) and in a similar way of the yield strength correlation methods:

$$\sigma_u = \beta_1 \frac{P_m}{t^2} + \beta_2 \quad (2)$$

where:

$\beta_1$  and  $\beta_2$  are correlation coefficients obtained in the linear regression.  
 $t$  is the specimen thickness.

Maximum load method balanced with the displacement  $u_m$  (see Figure 6): the previous maximum load method shows generally high deviations in the correlations. Introducing the displacement  $u_m$  (displacement where the SPT curve reaches the maximum load  $P_m$ ) in the correlation equation (see equation (3)), the accuracy of the correlations is significantly improved.

$$\sigma_u = \beta_1 \frac{P_m}{t u_m} + \beta_2 \quad (3)$$

Intersections' method (see Figure 6): based on the evidence of damage initiated in displacements prior to the maximum load  $P_m$ , some researchers introduced this alternative correlation method, which uses the punch load  $F_i$  at a fixed punch displacement of 0.645 mm. To standardize the nomenclature of this article, this punch load  $F_i$  is identified here as  $P_i$ . This load  $P_i$  is correlated linearly with the ultimate tensile strength following the equation (4):

$$\sigma_u = \beta_1 \frac{P_i}{t^2} \quad (4)$$

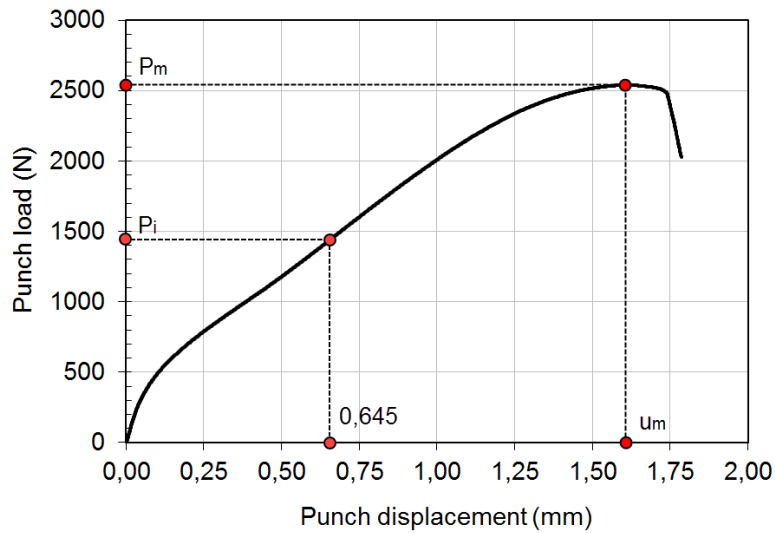


**Figure 6.** Data used from SPT curve to apply the maximum load method, the balanced method and the Intersections' method

In order to improve the accuracy of the ultimate tensile strength, an alternative correlation method, known as the  $Slope_{min}$  method, was introduced [20]. This method used the minimum slope of the zone III of the SPT curve ( $Slope_{min}$ ) instead of the punch loads  $P_m$  or  $P_i$  used in the previous methods, and it showed a good accuracy.

Although there is a lot of research focused on the understanding of the SPT behavior and the influence of the mechanical properties on the shape of the SPT curve, there is no numerical research that systematically studied the influence of each mechanical property over a wide range of values. In order to fill this gap, this article, focused on the simulation of SPT curves for a wide selection of hypothetical materials by means of the finite element method (FEM), shows the influence of the mechanical properties on all the correlation methods previously described.

## 2 Methodology and materials

A database of hypothetical materials was created to cover the mechanical properties of the most common metallic alloys used in load-supporting structures. The strain hardening for the hypothetical materials was simulated with the Ramberg-Osgood hardening law [21] (see equation (5)):

$$\varepsilon_{true} = \frac{\sigma_{true}}{E} + \varepsilon_{offset} \left( \frac{\sigma_{true}}{\sigma_y} \right)^n \quad (5)$$

where:

$\varepsilon_{offset} = 0.002$  is the plastic strain of the offset yield point,

$\sigma_{true}$  is the true stress,

$\varepsilon_{true}$  is the true strain,

$E$  is the Young's modulus,

$\sigma_y$  is the yield strength,

$n$  is the hardening coefficient.

Fourteen different Young's modules were selected in a range from 40 GPa to 240 GPa. The yield strength had different ranges depending on the value of the Young's modulus (Table 1 shows these ranges). And finally, the strain hardening was characterized with the hardening coefficient  $n$ , with four values from 5 to 30. The combinations generated 472 hypothetical materials. The influence of the Poisson ratio was not considered because of it was analyzed in a previous research [8], showing no significant influence on the SPT behavior for the structural-metallic-material typical values (0.25 to 0.35). Thus, the Poisson ratio was fixed in the midpoint of the previous range:  $\nu = 0.30$ .

**Table 1.** Mechanical properties of the hypothetical materials

$E$ (GPa)	$\sigma_y$ (MPa)	$n$	Number of materials
40, 50	50, 150, 250, 350, 450	5, 7, 12, 30	40
60, 70, 80	50, 150, 250, 350, 450, 550, 650, 750	5, 7, 12, 30	96
90, 100, 120, 140, 160	50, 250, 450, 650, 850, 1050, 1250, 1450	5, 7, 12, 30	160
180, 200, 220, 240	50, 250, 450, 650, 850, 1050, 1250, 1450, 1650, 1850, 2050	5, 7, 12, 30	176
<b>Total number of hypothetical materials</b>			<b>472</b>

Note: The offset yield point was set at a plastic strain of 0.2% in all the hypothetical materials ( $\varepsilon_{offset} = 0.002$ )

The software selected for this FEM analysis was ANSYS Mechanical, and the geometry for the parts of the SPT assembly was the next (see Figure 1 for symbols' identification):

$$R_d = 2.0 \text{ mm}$$

$$R_p = 1.25 \text{ mm}$$

$$t = 0.50 \text{ mm}$$

$$r = 0.50 \text{ mm}$$

To obtain the  $Slope_{UL}$ ,  $Slope_{ini}$  and  $Slope_{min}$  in the SPT's, the same process introduced in previous research is used to follow a standardized method [8,16,20].

### 3 Numerical analyses

ANSYS Mechanical was used to perform the FEM simulations of the SPT for the hypothetical materials. The model was simplified to an axisymmetric 2D simulation. All the parts were meshed with quadratic quadrilateral elements (Quad8) and quadratic triangles (Tri6). Specimen mesh was generated with a global seed of 0.10 mm and a local refinement in the center of the disk of 0.01 mm. Hemispherical punch was meshed with a global seed of 0.20 mm and a local refinement for the contact region with the specimen during the test of 0.02 mm. Contact behavior of all parts were introduced as frictional ( $\mu = 0.18$ ) and symmetrical with a pinball region of 0.3 mm. Stiffness of the hemispherical punch and the upper and lower dies were introduced as rigid bodies. The material behavior for the specimen was characterized as isotropic elasticity (Young's modulus and Poisson ratio) and tabular isotropic plasticity (yield strength and strain hardening). The strain hardening was simulated with a tabular data of plastic strain and stress following a Ramberg-Osgood hardening law (see equation (5)). The simulation of the SPT was performed up to a punch displacement of 0.70 mm with an unloading-loading cycle initiated at punch displacement of 0.1 mm to obtain the  $Slope_{UL}$  (see Figure 7). Figure 8 shows a general and a detail view of the FEM model.

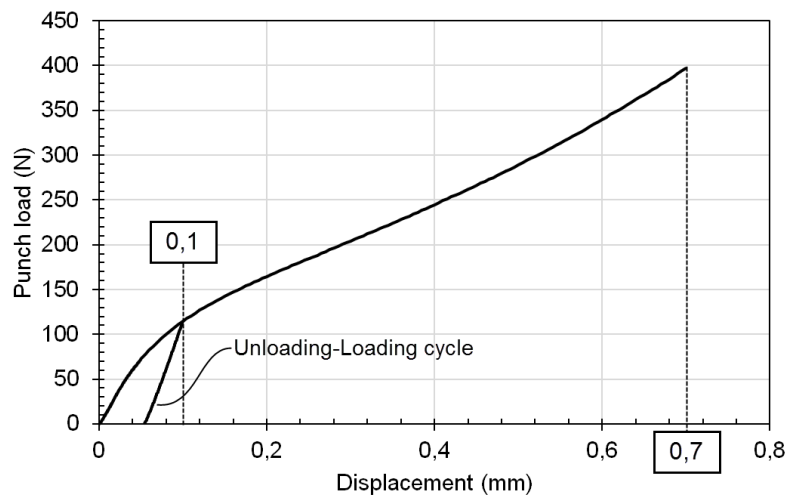


Figure 7. SPT curve obtained with the FEM simulations

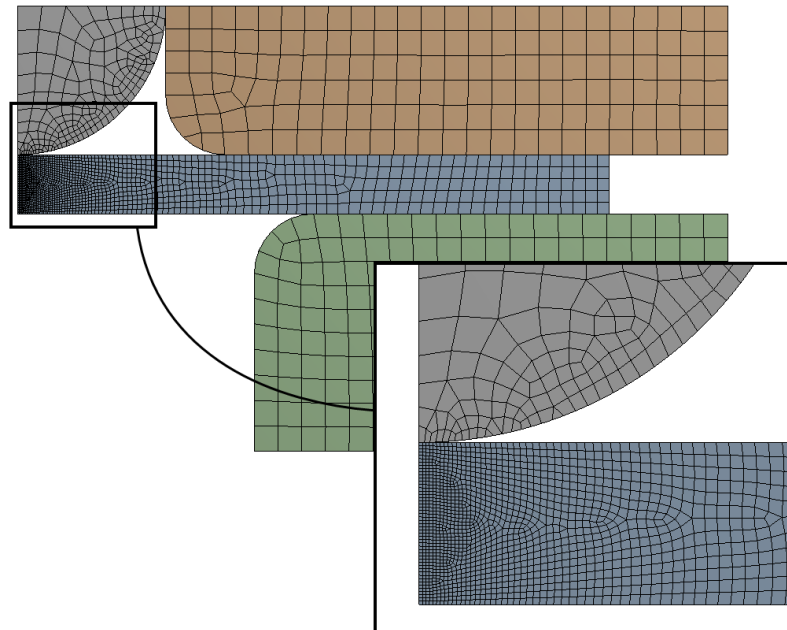
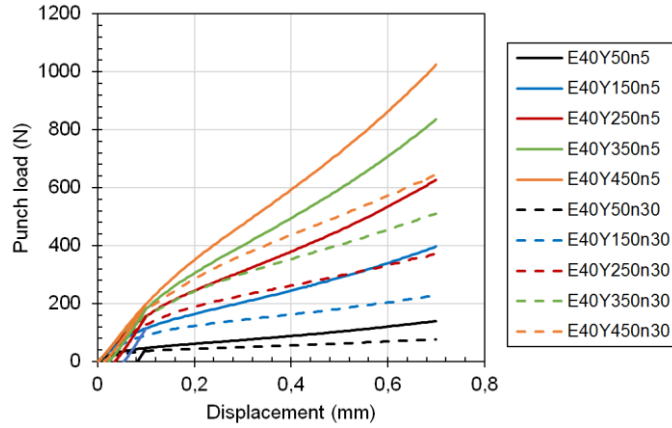


Figure 8. FEM model

Figure 9 shows the SPT curves for the hypothetical materials with a Young's modulus of 40 GPa, and the selected ranges for the yield strength and the hardening coefficient  $n$ . The SPT curves are identified with the acronyms "E<sub>xxx</sub>Y<sub>xxxn</sub>xx", each one representing the mechanical properties of the material ( $E$ , the Young's modulus;  $Y$ , the yield strength; and  $n$  the hardening coefficient). The numbers next to each one represent the value of each mechanical property. Figure 10 represents a small selection of ten SPT curves of the 472 performed simulations.

The following correlation methods were applied to the 472 SPT curves:

- $Slope_{ini}$  method (Young's modulus correlation).
- $Slope_{UL}$  method (Young's modulus correlation).
- Mao's method (yield strength correlation).
- CEN's method (yield strength correlation).
- Offset  $t/10$  method (yield strength correlation).
- $Slope_{ini}$  method (yield strength correlation).
- Intersections' method (ultimate tensile strength correlation).
- $Slope_{min}$  method (ultimate tensile strength correlation).



**Figure 9.** SPT curve for hypothetical materials E40 ( $n = 5$  and  $n = 30$ )

### 3.1 Young's modulus analysis

Figure 10 shows the linear regressions and the equations obtained in the estimation of the Young's modulus with the  $Slope_{ini}$  and the  $Slope_{UL}$  methods. The  $Slope_{ini}$  method showed a clear pattern which predicts a dependency of this correlation method with more than one mechanical property. This fact was analyzed with more detail in the next section. The  $Slope_{UL}$  method showed more accuracy and less dependency with other mechanical properties. The normalized root-mean-square deviation (NRMSD) was used to quantify the scattering of each correlation method (see equation (6)):

$$NRMSD = 100 \times \sqrt{\frac{\sum_{j=1}^m \sum_{i=1}^{n_j} \left[ \frac{E_i - E_j}{E_j} \right]^2}{n}} \quad (6)$$

where:

$E_i$  is the Young's modulus estimated with the regression curves included in Figure 10,

$E_j$  is the Young's modulus pre-defined in the simulations,

$n_j$  is the number of hypothetical materials with the same pre-defined Young's modulus,

$m$  is the number of different Young modules pre-defined in the simulations,

$n$  is the number of hypothetical materials ( $n = \sum_{j=1}^m n_j$ ).

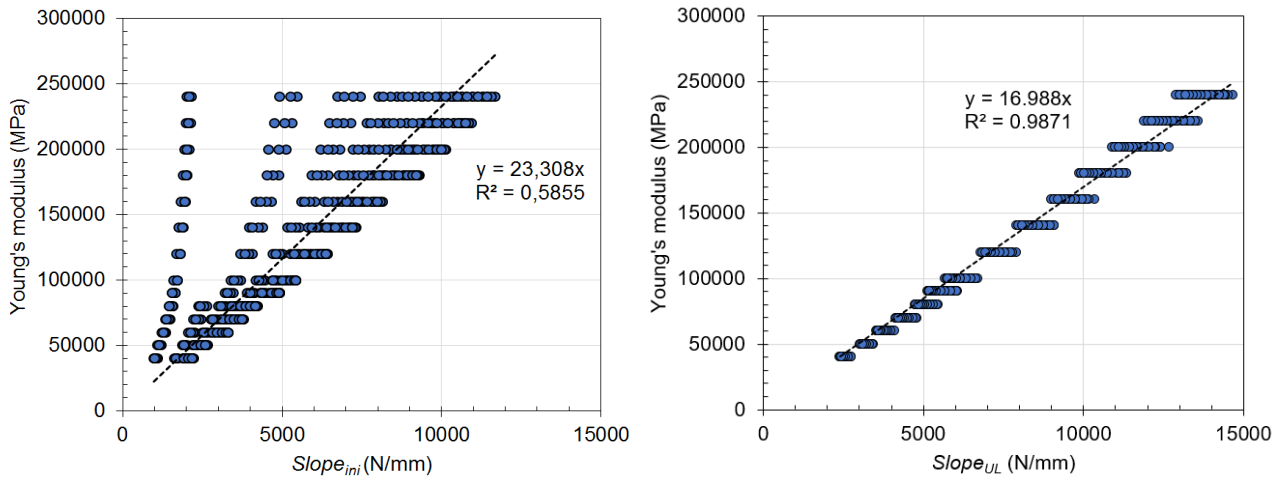


**Figure 10.**  $Slope_{ini}$  and  $Slope_{UL}$  methods to estimate the Young's modulus

Figure 11 shows that the scattering was significantly reduced with the  $Slope_{UL}$  method. This fact was demonstrated in a previous research [8].

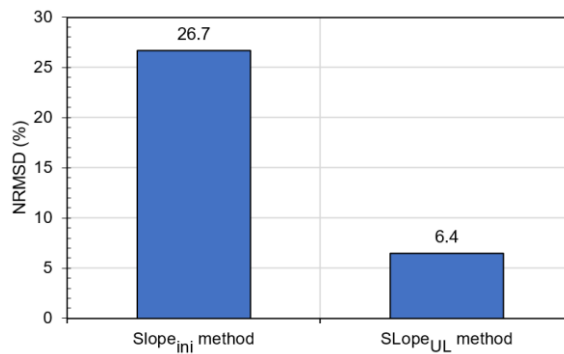


**Figure 11.** NRMSD in the correlation methods for the Young's modulus estimation

### 3.2 Yield strength analysis

Figure 12 and Figure 13 show the correlations for the hypothetical materials with the methods used to estimate the yield strength with the SPT. Figure 14 shows the NRMSD obtained for each correlation method.  $Slope_{ini}$  method showed the highest scattering and the most fitted correlation was obtained with the CEN's method.

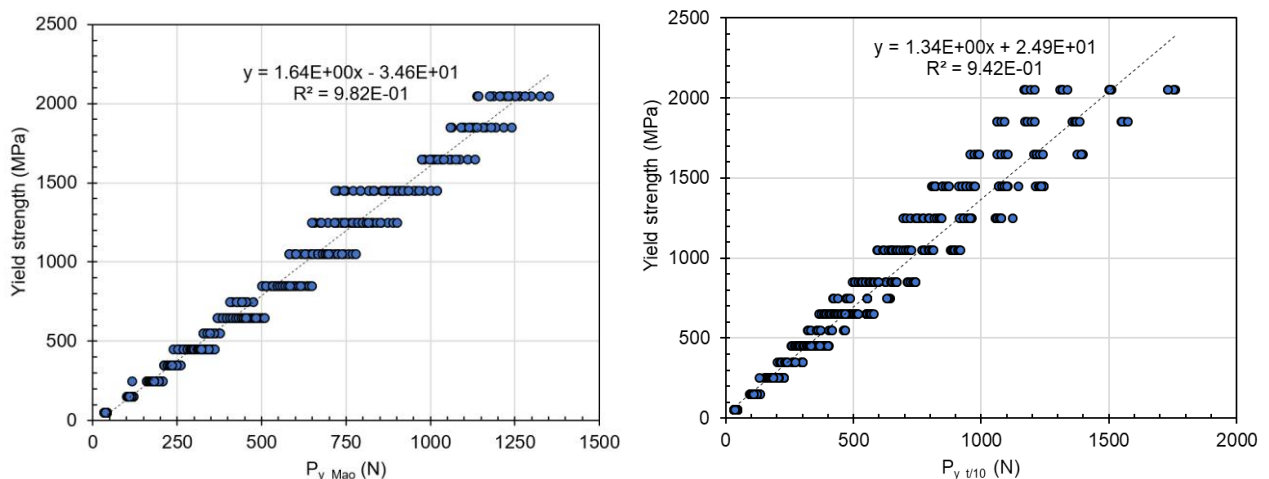


**Figure 12.** Mao's (left) and t/10 offset (right) methods

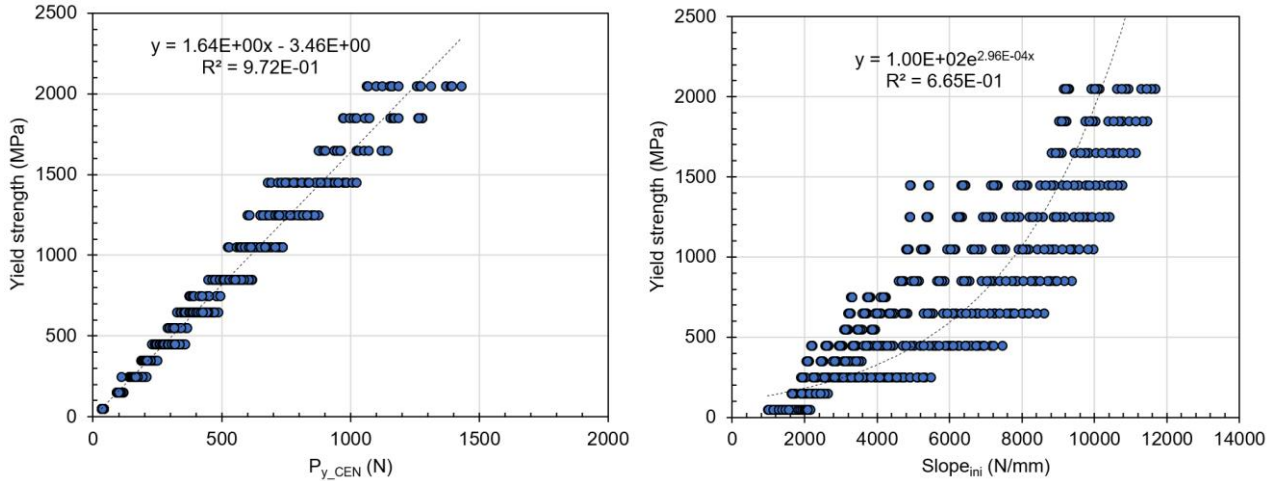


**Figure 13.** CEN's (left) and  $Slope_{ini}$  (right) methods

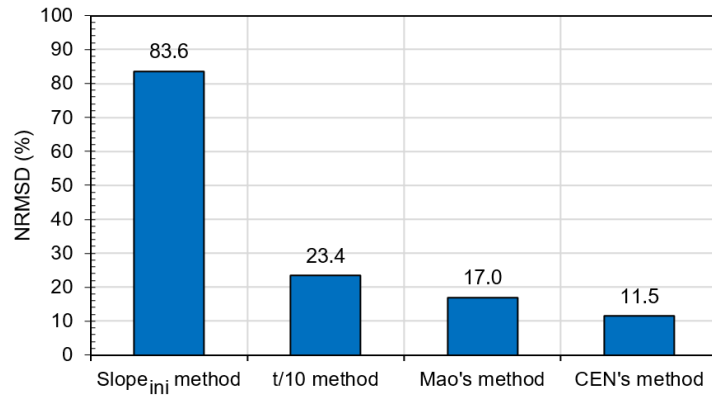


**Figure 14.** NRMSD in the correlation methods for the yield strength estimation

The scattering showed in the previous correlations was generated by the dependencies of each correlation method with multiple mechanical properties (not only with the yield strength). Figure 15 to Figure 19 show a more detailed representation of the results. Mao's method showed dependency with Young's modulus and the hardening coefficient  $n$ , but with similar sensitivity. Thus, it is difficult to discern dependencies in the specific case of the Mao's method.  $t/10$  offset and CEN's methods presented a clear dependency with the hardening coefficient  $n$  and less sensitivity to the Young's modulus. This low Young's modulus sensitivity was deduced due to the high values of the coefficient of determination  $R^2$  obtained on each linear regression. An interesting conclusion obtained from these figures is that the coefficient  $\alpha_2$  (see equation (1)) generally used in the experimental correlations is generated due to the dependency with the strain hardening. If this dependency is included in the coefficient  $\alpha_1$ ,  $\alpha_2$  is null.

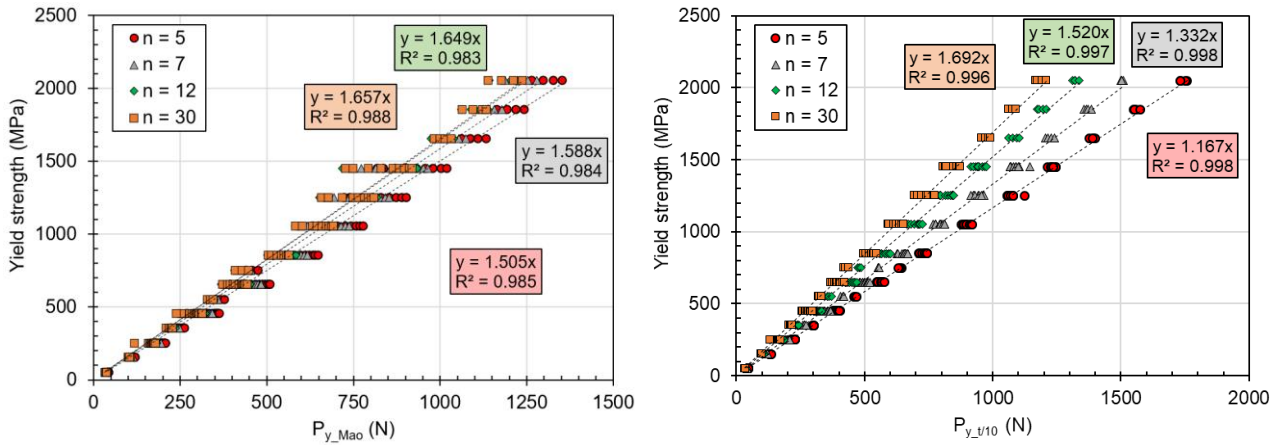


Figure 15. Mao's (left) and t/10 offset (right) methods

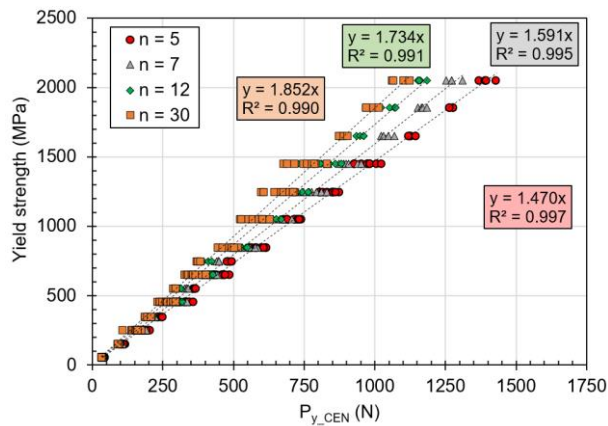


Figure 16. CEN's method

Figure 17, Figure 18 and Figure 19 show the dependencies of the  $Slope_{ini}$  method with the mechanical properties of the hypothetical materials. This correlation method was very sensitive to the Young's modulus and the yield strength. The influence of the hardening coefficient  $n$  was shown in the coefficient of determination ( $R^2$ ) of each regression (included in the mentioned figures). The high values of  $R^2$  showed that this correlation method is less affected by the hardening coefficient  $n$ .

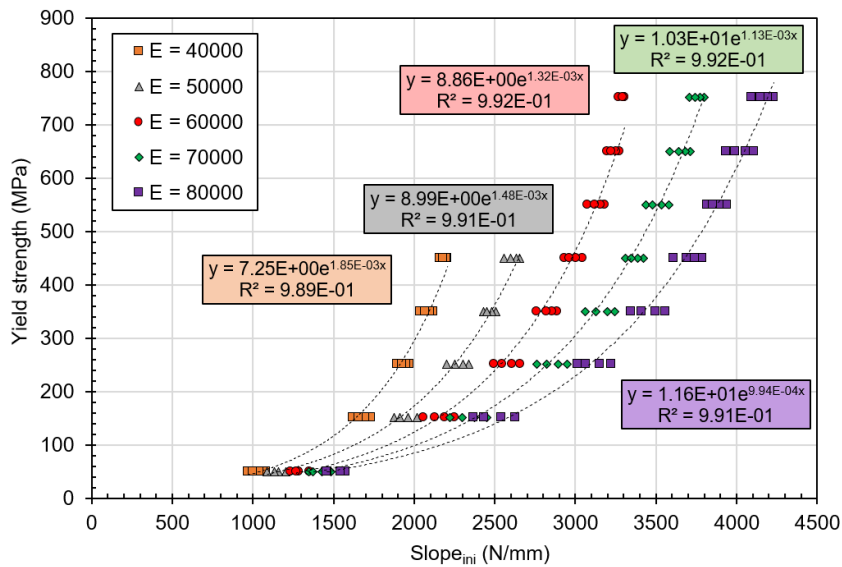


Figure 17.  $Slope_{ini}$  method

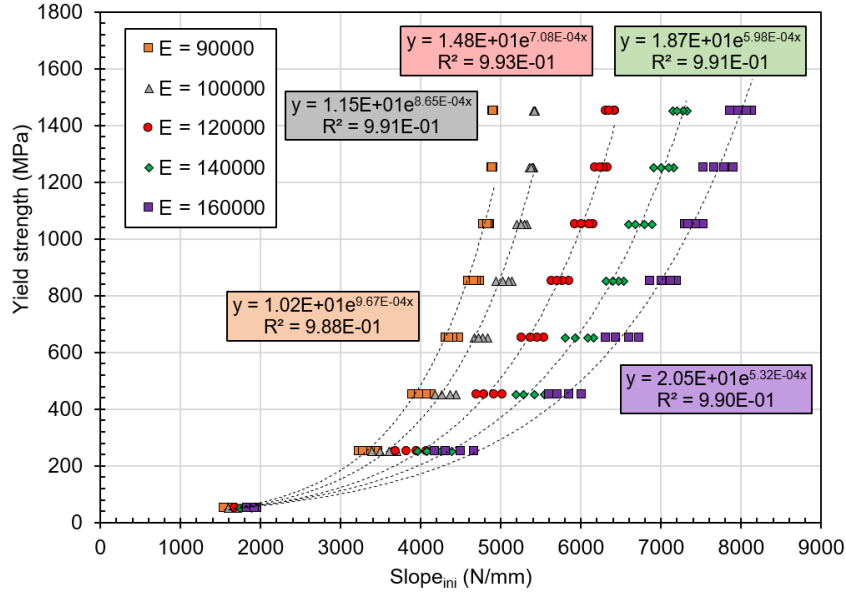


Figure 18.  $Slope_{ini}$  method

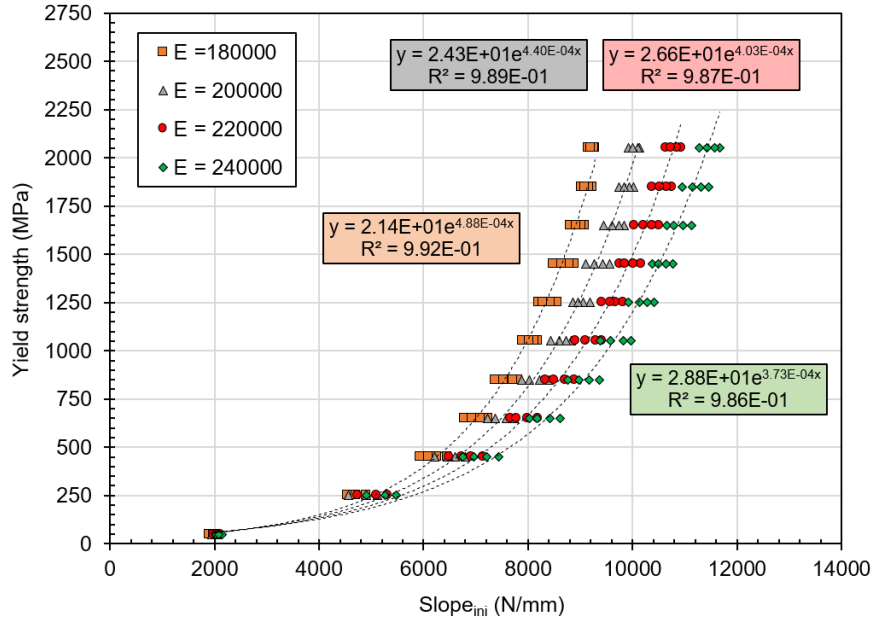
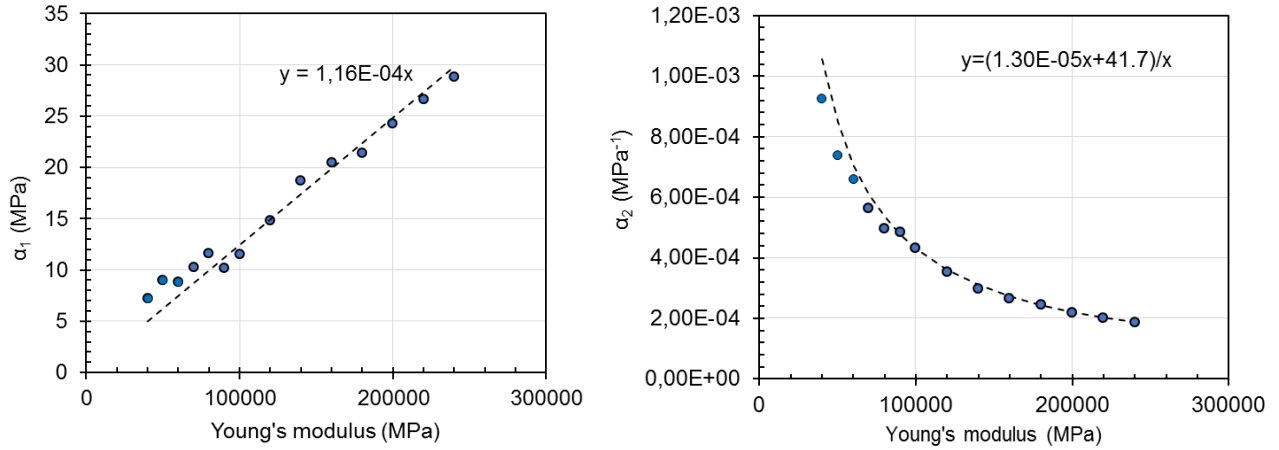


Figure 19.  $Slope_{ini}$  method

To take into consideration these multiple dependencies, regression coefficients of each correlation curve were plotted versus its appropriate pre-defined mechanical property. For the  $Slope_{ini}$  method, an exponential regression curve was introduced to correlate the  $Slope_{ini}$  with the yield strength [16] (see equation (7)). Figure 20 represents the coefficients  $\alpha_1$  and  $\alpha_2$  versus the Young's modulus and the appropriate regression equations obtained with *Matlab Curve Fitting Tool* using the non-linear least squares method.

$$\sigma_y = \alpha_1 \cdot e^{\alpha_2 \cdot \frac{Slope_{ini}}{t}} \quad (7)$$



**Figure 20.** Dependencies of the exponential regression coefficients in the  $Slope_{ini}$  method with the Young's modulus

Introducing these dependencies with the Young's modulus in the exponential regression of the  $Slope_{ini}$  method, the next equation (8) was obtained:

$$\sigma_y = 1.16 \cdot 10^{-4} \cdot E \cdot e^{\frac{1.3 \cdot 10^{-5} E + 41.7 \cdot Slope_{ini}}{E} t} \quad (8)$$

A linear regression between the yield load  $P_y$  and the pre-defined yield strength is presented in Figure 15 for the  $t/10$  offset method, showing a dependency with the hardening coefficient  $n$ . Equation (9) shows a generic representation of the linear regression established for this method where coefficient  $\alpha_2$  is considered null as indicated above. Figure 21 shows the dependency of the coefficient  $\alpha_1$  of the equation (9) (obtained from Figure 15) and the hardening coefficient  $n$ .

$$\sigma_y = \alpha_1 \cdot \frac{P_y}{t^2} \quad (9)$$

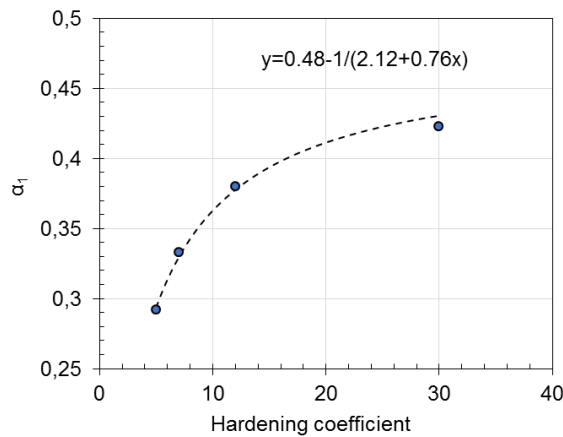


**Figure 21.** Dependency of the linear regression coefficient  $\alpha_1$  in the  $t/10$  offset method with the hardening coefficient  $n$

Introducing this dependency with the hardening coefficient  $n$  in the equation (9), the next equation for the yield strength estimation with the  $t/10$  offset method was obtained:

$$\sigma_y = \left( 0.48 - \frac{1}{2.12 + 0.76 \cdot n} \right) \cdot \frac{P_y}{t^2} \quad (10)$$

The CEN's method uses a linear regression in a similar way than the t/10 offset method. Thus, the equation (9) is a generic equation applicable to the CEN's method. Figure 22 shows the dependency of the linear regression coefficient  $\alpha_l$  with the hardening coefficient  $n$ .

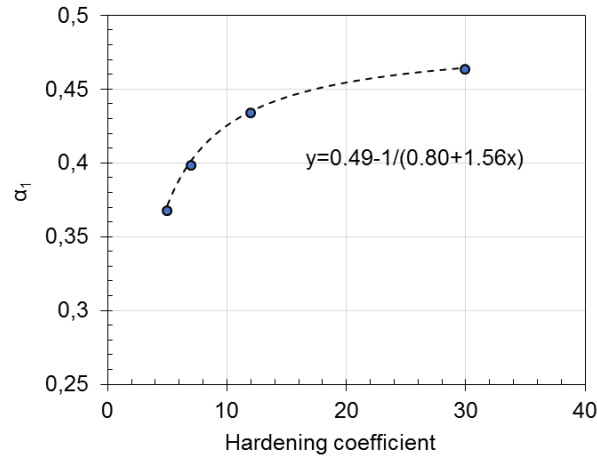


**Figure 22.** Dependency of the linear regression coefficient  $\alpha_l$  in the CEN's method with the hardening coefficient  $n$

The equation (11) shows the correlation for the CEN's method introducing the hardening coefficient  $n$ .

$$\sigma_y = \left( 0.49 - \frac{1}{0.80 + 1.56 \cdot n} \right) \cdot \frac{P_y}{t^2} \quad (11)$$

Finally, a similar analysis was done for the Mao's method, using the generic equation (9). Figure 23 shows the dependency of the linear regression coefficient  $\alpha_l$  with the hardening coefficient  $n$ , and the equation (12) shows the correlation equation.

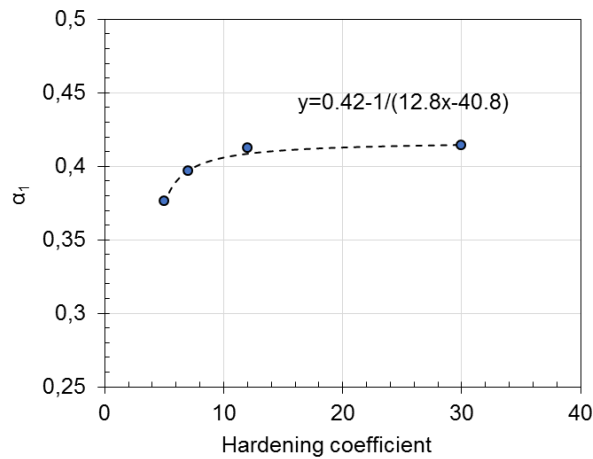


**Figure 23.** Dependency of the linear regression coefficient  $\alpha_l$  in the Mao's method with the hardening coefficient  $n$

$$\sigma_y = \left( 0.42 - \frac{1}{12.8 \cdot n - 40.8} \right) \cdot \frac{P_y}{t^2} \quad (12)$$

Figure 24 shows the NRMSD obtained previously with regression equations (non-corrected correlations "NC") and the values obtained with the improved regression equations (8),(10),(11) and (12) (improved with the mechanical

properties “C with MP”). The correlation methods improved their scattering, but it is significant the improvement reached by the  $Slope_{ini}$  method when the influence of Young’s modulus was introduced in the regression.

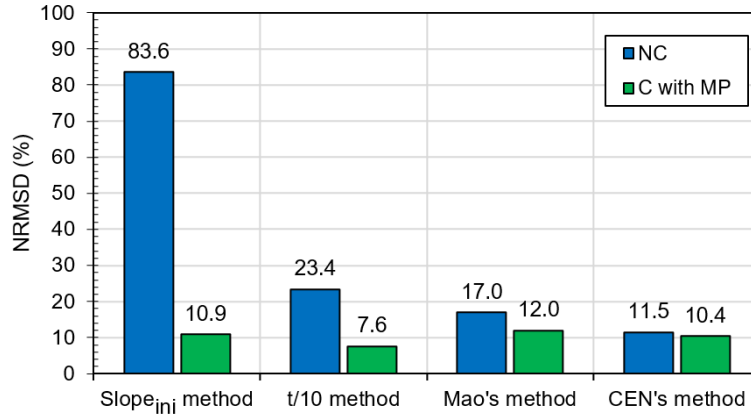


**Figure 24.** NRMSD in the correlation methods for the yield strength estimation

The improved correlation equations (8), (10), (11) and (12) for the yield strength estimation with the SPT needed the use of mechanical properties which had to be obtained by another method.  $Slope_{ini}$  method depended on the Young’s modulus and the other three methods (t/10 offset, Mao’s and CEN’s methods) depended on the hardening coefficient  $n$ .

The easiest way to calculate the hardening coefficient  $n$  with the SPT was introduced in a previous research [20] with the use of the Kamaya equation (13) [22]. It was used to obtain an equivalent hardening coefficient  $n$  from the yield strength and the engineering ultimate tensile strength of the material.

$$n = 3.93 \left( \ln \left( \frac{\sigma_{u\_eng}}{\sigma_y} \right) \right)^{-0.754} \quad (13)$$

Considering that the ultimate tensile strength can be estimated with the Intersections’ method with the equation (4), and combining it with the equation (13) next formula was obtained:

$$n = 3.93 \left( \ln \left( \frac{\beta_1 \frac{P_i}{t^2}}{\sigma_y} \right) \right)^{-0.754} \quad (14)$$

Equation (14) was introduced in equations (10), (11) and (12) to substitute the hardening coefficient  $n$  and to obtain the improved correlation equations (15), (16) and (17) for the t/10 offset, CEN’s and Mao’s methods using only the SPT data. The main problem of these equations is that it is not possible to analytically estimate the yield strength from them. Thus, numerical methods have to be used to estimate the yield strength. In this article, the Newton’s numerical method was used.

$$\sigma_y = \left( 0.48 - \frac{1}{2.12 + 0.76 \cdot \left[ 3.93 \left( \ln \left( \frac{\beta_1 \frac{P_i}{t^2}}{\sigma_y} \right) \right)^{-0.754} \right]} \right) \cdot \frac{P_{y\_t/10}}{t^2} \quad (15)$$

$$\sigma_y = \left( 0.49 - \frac{1}{0.80 + 1.56 \cdot \left[ 3.93 \left( \ln \left( \frac{\beta_1 \frac{P_i}{t^2}}{\sigma_y} \right) \right)^{-0.754} \right]} \right) \cdot \frac{P_{y\_CEN}}{t^2} \quad (16)$$

$$\sigma_y = \left( 0.42 - \frac{1}{12.8 \cdot \left[ 3.93 \left( \ln \left( \frac{\beta_1 \frac{P_i}{t^2}}{\sigma_y} \right) \right)^{-0.754} \right] - 40.8} \right) \cdot \frac{P_{y\_Mao}}{t^2} \quad (17)$$

The  $Slope_{ini}$  method depends on the Young's modulus (see equation 8). Combining the regression equation shown in the Figure 10 for the  $Slope_{UL}$  method, with the equation (8) of the  $Slope_{ini}$  method, the equation (18) was obtained.

$$\begin{aligned} \sigma_y &= 1.16 \cdot 10^{-4} \cdot (16.988 \cdot Slope_{UL}) \cdot e^{\frac{1.3 \cdot 10^{-5} (16.988 Slope_{UL}) + 41.7 \times Slope_{ini}}{(16.988 Slope_{UL})} \times \frac{Slope_{ini}}{t}} = \\ &= \frac{Slope_{UL}}{507.46} \cdot e^{\frac{1.3 \cdot 10^{-5} Slope_{UL} + 2.4 \times Slope_{ini}}{Slope_{UL}} \times \frac{Slope_{ini}}{t}} \end{aligned} \quad (18)$$

Figure 25 shows the NRMSD obtained from the equations (15), (16), (17) and (18) which uses only data obtained from the SPT ("C with SPT"). CEN's, offset  $t/10$  and Mao's method showed the best fitted results, but the complexity of the equations (15), (16) and (17) made them hard to apply. Nevertheless, the  $Slope_{ini}$  method, weighed with the Young's modulus by the  $Slope_{UL}$  method, was easier to calculate with the SPT curve.

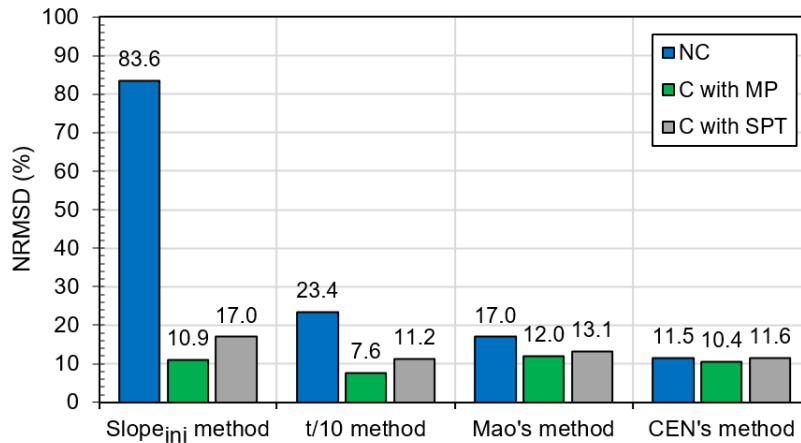


**Figure 25.** NRMSD in the correlation methods for the yield strength estimation

Although the non-improved ("NC") CEN's method showed a NRMSD of 11.5%, lower than the value obtained by the "C with SPT"  $Slope_{ini}$  method (17.0%), these calculations have been established for a wide selection of hypothetical materials with Young's modulus from 40 GPa to 240 GPa. When the characterization study is centered in alloys with similar Young's modulus, the  $Slope_{ini}$  method has been the most accurate method due to its low dependency with the strain hardening of the material [16]. In a real mechanical characterization study with the SPT

is easier to fix the Young's modulus of the tested materials than other mechanical properties like the strain hardening which can be altered by cold-working or thermal treatments applied in the same material.

### 3.3 Ultimate tensile strength analysis

Hypothetical material simulations used in this research did not include damage properties. Thus, the maximum load method and the balanced maximum load method were not possible to be analyzed. For the Intersections' method, Figure 26 shows the linear regression obtained between the ultimate tensile strength of the hypothetical materials and the value  $P_i$ . The ultimate tensile strengths were deduced from the pre-defined hardening coefficient  $n$  and the pre-defined yield strength using the Kamaya equation (13).

The alternative  $Slope_{min}$  method for the estimation of the ultimate tensile strength uses the correlation equation (19) [20]. This correlation method is dependent with the yield strength. Thus, it needs to be combined with the  $Slope_{mi}$  method (equation (18)) to find the ultimate tensile strength. The coefficients  $A$ ,  $B$  and  $C$  of this equation were obtained with the *Matlab Curve Fitting Tool* [20] using the non-linear least squares method.

$$\ln \left[ \frac{\sigma_u}{\sigma_y} \right] = 6.142 \left[ \frac{Slope_{min} - (A\sigma_y^2 + B\sigma_y)}{C\sigma_y} \right]^{1.326} \quad (19)$$

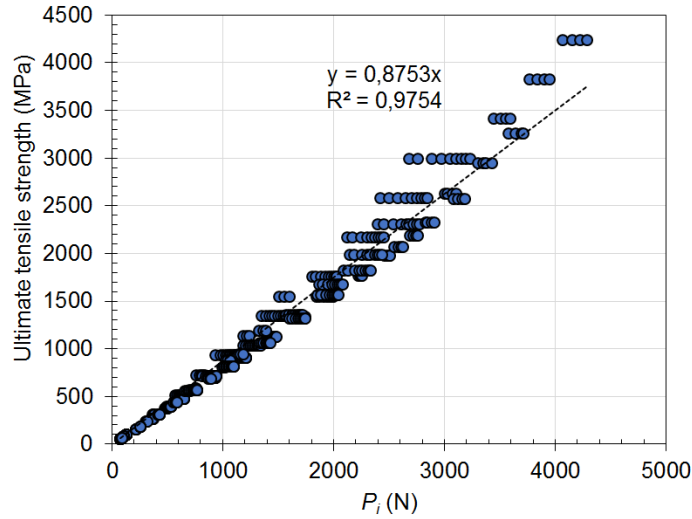


**Figure 26.** Intersections' method correlation

The influence of Young's modulus in the parameters  $A$ ,  $B$  and  $C$  of the equation (19) was also analyzed with the *Matlab Curve Fitting Tool*. Figure 27 shows the regression surface obtained for the hypothetical materials with a pre-defined Young's modulus of 40 GPa. Extending this analysis to the rest of the hypothetical materials, only the parameter  $A$  of the equation (19) showed a dependency with the Young's modulus (see Figure 28). Thus, the equation (19) was established as follows for the hypothetical materials:

$$\ln \left[ \frac{\sigma_u}{\sigma_y} \right] = 6.142 \left[ \frac{Slope_{min} - \left( \frac{20.74 - 1.36 \cdot 10^{-4} E}{E} \sigma_y^2 + 1.066 \cdot \sigma_y \right)}{7.2 \cdot \sigma_y} \right]^{1.326} \quad (20)$$

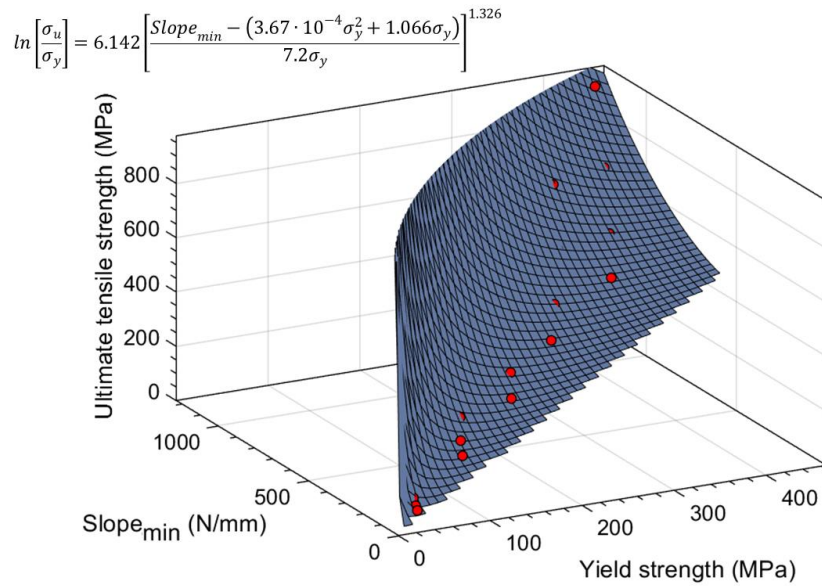


**Figure 27.**  $Slope_{min}$  correlation surface for the hypothetical materials with Young's modulus of 40 GPa

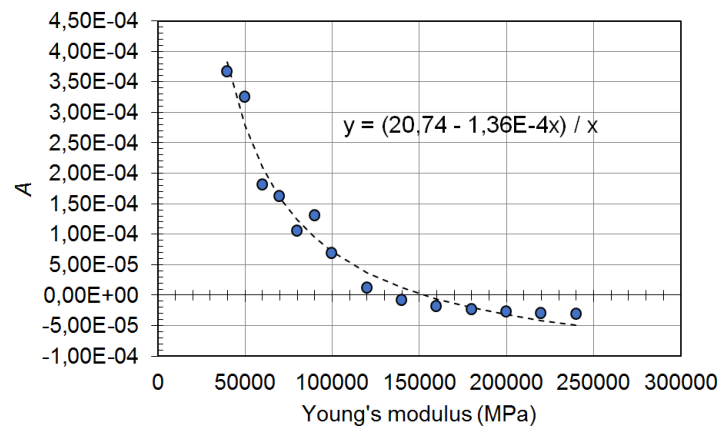


**Figure 28.** Influence of the Young's modulus in the coefficient A of the equation (19)

In the application of the  $Slope_{min}$  method with the improved equation (20), the Young's modulus was estimated with the  $Slope_{UL}$  method obtained in the Figure 10. Figure 29 shows a comparison between the Intersections' and the  $Slope_{min}$  correlation methods plotting the ultimate tensile strength used in the simulations with the values estimated with each correlation method. The NRMSD included in Figure 30 showed that the  $Slope_{min}$  method corrected with the  $Slope_{UL}$  method had less scattering than the Intersections' method.

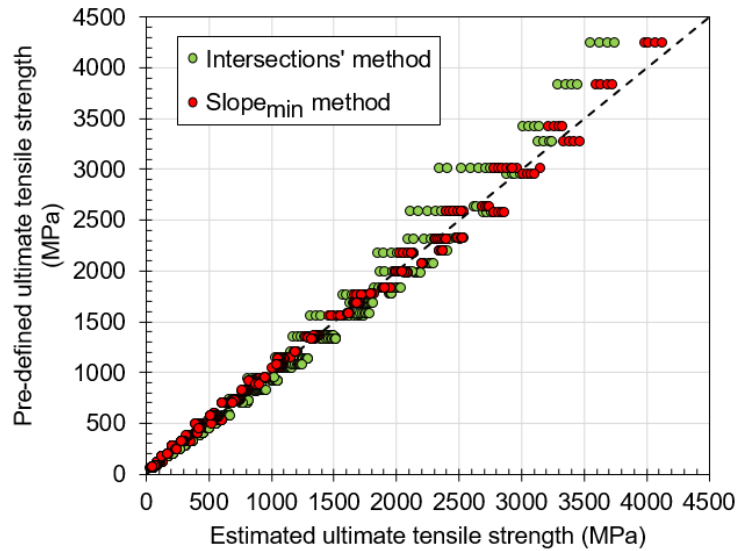


**Figure 29.** Comparison of the pre-defined vs. estimated ultimate tensile strengths with the intersections' and  $Slope_{min}$  methods

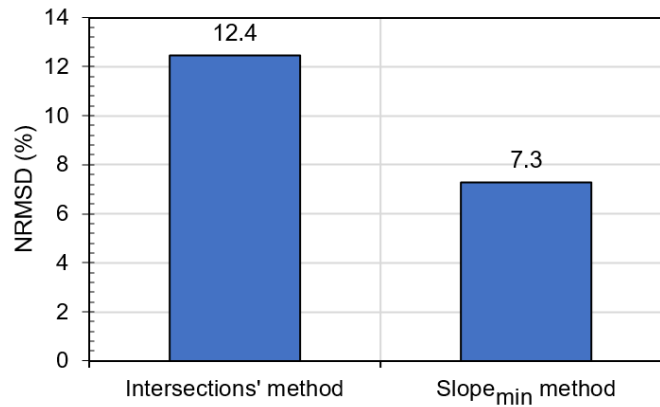


**Figure 30.** NRMSD for the ultimate tensile strength correlation methods

## 4 Conclusions

In this investigation, a systematic FEM analysis was performed to evaluate the influence of each mechanical property in the correlation methods used in the SPT. After this study the next conclusions were established:

- a) All the correlation methods used in the SPT to the calculation of the Young's modulus, yield strength and ultimate tensile strength are dependent with more than one mechanical property.
- b) These multiple dependencies were analyzed, and the correlation equations were modified to include this behavior and to improve their scattering. Equations (21), (22) and (23) show these equations with the regression coefficients which have to be calculated numerically or experimentally:
  1. Mao, Offset  $t/10$  and CEN's methods (coefficients  $\alpha_1$ ,  $\alpha_2$ ,  $\alpha_3$  and  $\beta_1$ ):

$$\sigma_y = \left( \alpha_1 - \frac{1}{\alpha_2 + \alpha_3 \cdot \left[ 3.93 \left( \ln \left( \frac{\beta_1 P_i}{\sigma_y t^2} \right) \right)^{-0.754} \right]} \right) \cdot \frac{P_y}{t^2} \quad (21)$$

2. *Slope<sub>ini</sub>* method (coefficients  $\alpha_1$ ,  $\alpha_2$  and  $\alpha_3$ ):

$$\sigma_y = \frac{Slope_{UL}}{\alpha_1} \cdot e^{\frac{\alpha_2 \cdot Slope_{UL} + \alpha_3 \cdot Slope_{ini}}{Slope_{UL}} \times \frac{Slope_{ini}}{t}} \quad (22)$$

3. *Slope<sub>min</sub>* method (coefficients  $\beta_1$ ,  $\beta_2$ ,  $\beta_3$  and  $\beta_4$ ):

$$\ln \left[ \frac{\sigma_u}{\sigma_y} \right] = 6.142 \left[ \frac{Slope_{min} - \left( \frac{\beta_1 - \beta_2 E}{E} \sigma_y^2 + \beta_3 \cdot \sigma_y \right)}{\beta_4 \cdot \sigma_y} \right]^{1.326} \quad (23)$$

- c) For the yield strength calculation, the most fitted results were obtained with the t/10 offset method, but numerical methods had to be used to apply the improved equation. Nevertheless, the improved equation for the *Slope<sub>ini</sub>* method is easier to be applied.
- d) For the Mao's, offset t/10 and CEN's method, coefficient  $\alpha_2$  used in the correlation equation (1) is generated due to the influence of the strain hardening in the yield loads  $P_y$ . When this influence was considered in the correlation equation this coefficient  $\alpha_2$  was null.
- e) For the ultimate tensile strength calculation, the *Slope<sub>min</sub>* improved method showed less scattering than the Intersections' method.

## 5 Data availability

The raw/processed data required to reproduce these findings cannot be shared at this time as the data also forms part of an ongoing study.

## 6 References

- [1] M.P. Manahan, A.S. Argon, O.K. Harling. Mechanical behavior evaluation using the miniaturized disk bend test, Quaterly Progress Report on Damage Analysis and Fundamental Studies (1981) 82-103. DOE/ER-0046/8.
- [2] M.P. Manahan, A.S. Argon, O.K. Harling, The development of a miniaturized disk bend test for the determination of postirradiation mechanical properties, Journal of Nuclear Materials 103 & 104 (1981) 1545-1550.
- [3] M. Dooley, G.E. Lucas, J.W. Sheckherd, Small scale ductility tests, Journal of Nuclear Materials 104 (1981) 1533-1537. DOI: 10.1016/0022-3115(82)90818-2
- [4] G.E. Lucas, J.W. Sheckherd, G.R. Odette, S. Panchanadeeswaran, Shear punch tests for mechanical property measurements in TEM disc-sized specimens, Journal of Nuclear Materials 122 & 123 (1984) 429-434. DOI: 10.1016/0022-3115(84)90635-4.

- [5] J-M. Baik, J. Kameda, O. Buck, Small punch test evaluation of intergranular embrittlement of an alloy steel, *Scripta Metallurgica* 17 (1983) 1443-1447. DOI: 10.1016/0036-9748(83)90373-3.
- [6] H. Huang, M.L. Hamilton, G.L. Wire, Bend testing for miniature disks, *Nuclear Technology* 57 (1982) 234-242, DOI: 10.13182/NT82-A26286
- [7] E. Fleury, J.S. Ha, Small punch tests to estimate the mechanical properties of steels for steam power plant: I. Mechanical strength, *International Journal of Pressure Vessels and Piping* 75 (1998) 699-706, DOI: 10.1016/S0308-0161(98)00074-X.
- [8] J. Calaf-Chica, P. M. Bravo, M. Preciado, Improved correlation for the elastic modulus prediction of metallic materials in the Small Punch Test, *International Journal of Mechanical Sciences* 134 (2017) 112-122. DOI: 10.1016/j.ijmecsci.2017.10.006
- [9] X. Mao, H. Takahashi, Development of a further-miniaturized specimen of 3 mm diameter for TEM disk ( $\varnothing$  3 mm) small punch tests, *Journal of Nuclear Materials* 150 (1987) 42-52. DOI: 10.1016/0022-3115(87)90092-4.
- [10] A. Okada, M.L. Hamilton, F.A. Garner, Microbulge testing to neutron irradiated materials, *Journal of Nuclear Materials* 179-181 (1991) 445-448, DOI: 10.1016/0022-3115(91)90120-V.
- [11] Y. Ruan, P. Spatig, M. Victoria, Assessment of mechanical properties of the martensitic steel EUROFER97 by means of punch tests, *Journal of Nuclear Materials* 307-311 (2002) 236-239, DOI: 10.1016/S0022-3115(02)01194-7.
- [12] J. Kameda, R. Ranjan, Characterization of deformation and fracture behavior in amorphous and/or ceramic coatings and aluminum alloy substrates by small punch testing and acoustic emission techniques, *Materials Science and Engineering A* 183 (1994) 121-130, DOI: 10.1016/0921-5093(94)90896-6.
- [13] B. Ule, et al., Small punch test method assessment for the determination of the residual creep life of Service exposed components: outcomes from an interlaboratory exercise, *Nuclear Engineering and Design* 192 (1999) 1-11, DOI: 10.1016/S0029-5493(99)00039-4.
- [14] Comité Européen de Normalisation, Small punch test method for metallic materials, CWA 15627, Bruselas, Bélgica (2007).
- [15] M. Bruchhausen et al., European standard on small punch testing of metallic materials, *Proceedings of 5<sup>th</sup> International Small Sample Test Techniques Conference* (2018) 1-14.
- [16] J. Calaf-Chica, P. M. Bravo, M. Preciado, Development of an improved prediction method for the yield strength of Steel alloys in the Small Punch Test, *Materials & Design* 148 (2018) 153-166. DOI: 10.1016/j.matdes.2018.03.064
- [17] J. Calaf-Chica, Estudio y mejora de la correlación de propiedades mecánicas con los ensayos miniatura de punzonado, PhD thesis, University of Burgos (2018).
- [18] R. Hurst, K. Matocha, Where are we now with the european code of practice for small punch testing?, *Proceedings of the International Conference on Small Sample Test Techniques* (2012) 4-18.
- [19] E. Altstadt, et al., On the estimation of ultimate tensile stress from small punch testing, *International Journal of Mechanical Sciences* 136 (2018) 85-93, DOI: 10.1016/j.ijmecsci.2017.12.016.
- [20] J. Calaf-Chica, P.M. Bravo, M. Preciado, A new prediction method for the ultimate tensile strength of steel alloys with small punch test, *Materials* 11-9 (2018) 1492. DOI: 10.3390/ma11091491

- [21] W. Ramberg, W.R. Osgood, Description of stress-strain curves by three parameters, Technical Note 902, NACA, Washington DC, 1943.
- [22] M. Kamaya, Ramberg-Osgood type stress-strain curve estimation using yield and ultimate strengths for failure assessments, International Journal of Pressure Vessels and Piping 137 (2016) 1-12. DOI: 10.1016/j.ijvpv.2015.04.001.